ORGANOMETALLICS

Article

pubs.acs.org/Organometallics

Mechanistic Investigation on Scandium-Catalyzed C−H Addition of Pyridines to Olefins

Gen Luo,[†] Yi Luo,*[,†] Jingping Qu,[†] and Zhaomin Hou*[,†,‡]

[†]State Key Laboratory of Fine Chemicals, School of Pharmaceutical Science and Technology, Dalian University of Technology, Dalian 116024, People's Republic of China

[‡]Organometallic Chemistry Laboratory, RIKEN Advanced Science Institute, 2-1 Hirosawa, Wako, Saitama 351-0198, Japan

Supporting Information

ABSTRACT: This paper reports computational studies on the ortho alkylation of pyridines via C−H addition to olefins catalyzed by cationic half-sandwich rare-earth alkyl species. A detailed mechanism concerning the generation of catalytically active species and C−H addition has been computationally investigated at the molecular and electronic levels. The results support the mechanism based on experiments, which involves the initial generation of a metal pyridyl active species, followed by the coordination and insertion of an olefin and the subsequent pyridine C−H activation by a metal−carbon bond. The *o*-methyl sp^3 C−H activation product of α-picoline has been also calculated, and the results suggest that the sp^3 C−H activation product mainly results from the conversion of the sp^2 C−H activation product of α-picoline rather than from the direct reaction of the cationic species $(\eta^5\text{-}C_5Me_5)Sc(CH_2C_6H_4NMe_2\text{-}o)^+$ with α-picoline, and such a conversion is reversible. The reaction rate of the whole process is controlled by the generation of active species and an insertion step. The formation of the branched product is both kinetically and energetically favorable over that of the linear product, which is in agreement with the experimental observation. Both steric and electronic factors account for the regioselectivity. An analysis of energy decomposition provides new insights into the stability of the 1-hexene insertion transition states involved in such processes. A comparison between the successive olefin insertion and the C−H activation of pyridine has also been computationally carried out. In addition, it is predicted that the cationic scandium pyridyl species $(\eta^5\text{-}C_5Me_5)Sc(MeC_5H_3N)^+$ has a shorter induction period than the initial aminobenzyl analogue (precursor) $(\eta^5\text{-}C_5Me_5)Sc(CH_2C_6H_4NMe_2\text{-}o)^+$ for the initiation step of ethylene polymerization.

INTRODUCTION

Pyridine derivatives exist widely in pharmaceuticals, natural products, and functional materials.[1] In this context, the synthesis of alkyl-substituted pyridines through direct C−H functionalization of pyridine is of considerable importance.[2−6] Among all possible approaches, the catalytic C−H addition of pyridines to olefins is the most atom-economical way toward the synthesis of alkylpyridines. Previously, some transition-metal complexes[7−9] and rare-earth metallocenes[10] have been reported to catalyze the C−H addition of pyridines to olefins, but only with limited success in terms of selectivity and substrate scope.

The cationic half-sandwich rare-earth alkyl complexes have recently emerged as a new family of olefin polymerization catalysts, which show excellent activity and selectivity for the polymerization and copolymerization of a wide range of olefins, such as syndiospecific polymerization and copolymerization of styrene with ethylene, dienes, and other olefins.[11,12] Very recently, some of us disclosed that such cationic rare-earth alkyl complexes can also serve as excellent catalysts for highly efficient, ortho-selective C−H addition of pyridines to olefins, including α-olefins, styrenes, and conjugated dienes.[13] According to the experimental observations[13] and the results reported previously,[7−10] a plausible mechanism was proposed as shown in Scheme 1.[13] The whole process includes two main steps: (a) the generation of active species **D** via the reaction of cationic species **A** with pyridine and (b) the catalytic C−H addition of pyridine to olefin. However, many details such as the accessibility and the geometric and energetic aspects of these pathways, as well as the factors governing the activity and regioselectivity, remain unclear. Previously, computational studies on the catalytic hydroarylation of olefins were reported,[14−16] but most of them were limited to late-

Scheme 1. Possible Mechanism for Catalytic C−H Addition of Pyridines to Olefins Proposed on the Basis of Experiments

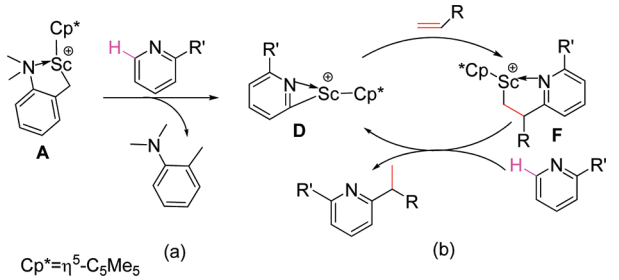

Received: February 23, 2012
Published: May 11, 2012

transition-metal-catalyzed reactions of benzene or its derivitives. Lin and Jordan et al. reported a theoretical study on zirconocene-catalyzed *o*-C−H addition of α-picoline to propene, which indicated that H_2 is important as a cocatalyst for this reaction and that the origin of the regioselectivity for 1,2-insertion of propene was due to steric effects while the regioselectivity for 2,1-insertion of vinyltrimethylsilane was due to electronic influence.[17]

During our computational studies on organometallic complexes,[18] we have carried out a series of theoretical calculations on olefin polymerization catalyzed by cationic rare-earth-metal complexes.[19] We have recently found that the mechanism of styrene−ethylene copolymerization catalyzed by a cationic half-sandwich scandium alkyl species is different from that involved in group 4 catalyst systems.[19d] In view of the fact that such a polymerization process is related to a Ln−C bond (Ln = rare-earth metal) insertion into olefin, we became interested in theoretical studies on the insertion of a C−H bond into olefins catalyzed by cationic rare-earth-metal complexes. In this work, we have computationally investigated the process shown in Scheme 1 at the molecular and electronic levels, with the purpose of disclosing the detailed mechanism and offering information on the development of new catalysts.

COMPUTATIONAL DETAILS

All calculations were performed with Gaussian 09 program.[20] The DFT method of B3PW91[21] was used for geometry optimizations and vibrational calculations. The 6-31G* basis set was used for C, H, and N atoms, and Sc atoms were treated by the Stuttgart/Dresden effective core potential (ECP) and the associated basis sets.[22] Each optimized structure was analyzed by harmonic vibrational frequencies obtained at the same level and characterized as a minimum (N_{imag} = 0) or a transition state (N_{imag} = 1). To obtain more reliable relative energies, a larger basis set and solvent effect with the CPCM model were considered. The single-point energies (in toluene solution with UFF atomic radii[23]) were calculated at the B3PW91/6-31+G**/SDD level for optimized structures. The free energies in toluene (used in experiment) solution were obtained from SCRF single-point calculations, and the gas-phase Gibbs free energy corrections were included. The strategy of performing solvation single-point calculations with a larger basis set on the geometry optimized with a smaller basis set is often used in the literature.[24]

RESULTS AND DISCUSSION

Generation of Active Species D. To investigate the step (a) shown in Scheme 1, the energy profile for the reaction of 2-ethylpyridine with cationic complex **A**, leading to catalytically active species **D**, has been computed. As shown in Figure 1, the coordination of 2-ethylpyridine to **A** forms complex **B**, which further goes through a four-center hydrogen transfer (HT) transition state, **TS1**, leading to **C** with the *o*-$Me_2NC_6H_4Me$ moiety. **C** could release *o*-$Me_2NC_6H_4Me$ to generate the catalytically active species **D**. **TS1** has a free energy barrier of 20.93 kcal/mol. The optimized structure of **TS1** is shown in Figure 2. As shown in this figure, C_α, Sc, $C_{\alpha'}$, and the transferring H construct a four-center structure, as suggested by the interatomic distances, viz. 2.401 (Sc···$C_{\alpha'}$), 2.254 (Sc···C_α), 1.455 ($C_{\alpha'}$···H), 1.433 ($C_{\alpha'}$···H), and 1.877 Å (Sc···H), as well as the C_α···Sc···$C_{\alpha'}$ angle of 76.2°. These geometrical features are similar to those involved in the reaction of methane with [Cp_2ScCH_3] (viz. the Sc···H distance of 1.90 Å and the H_3C···Sc···CH_4 angle of 73.5°)[25a] and suggest that a one-step σ-bond metathesis (σ-BM) process occurs via a four-center transition state structure. This step shows the typical σ-bond

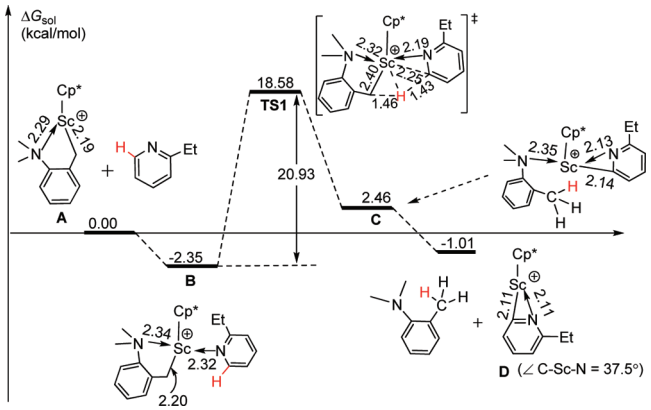

Figure 1. Energy profile (free energy in toluene solution) for the formation of active species **D** via the reaction of **A** with 2-ethylpyridine (distances in Å and angles in deg).

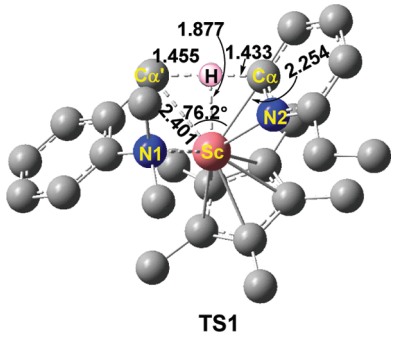

Figure 2. Optimized structure of transition state **TS1** (distances in Å and angles in deg). The hydrogens, except for the transferring H, are omitted for clarity.

metathesis mechanism,[25] but the catalytic hydroarylation reaction involving a late transition metal often occurs through an oxidative hydrogen migration (OHM) transition state showing a metal transformation from M^n to M^{n+2}.[16]

Insertion of Olefin into D and Subsequent C−H Bond Activation. The generated active species **D** could be involved in the catalytic cycle. The computed catalytic pathway for the reaction of 2-ethylpyridine with 1-hexene is shown in Figure 3. To investigate the regioselectivity, both 1,2- and 2,1-insertions of 1-hexene into the Sc−C bond of **D** were calculated. As shown in Figure 3, the 1,2-insertion process (black line) starts with the formation of complex **1,2-E** showing a 1,2-coordination of 1-hexene to the metal center. **1,2-E** goes through a four-center transition state, **1,2-TS2**, leading to intermediate **1,2-F** as an insertion product. **1,2-TS2** has a free energy barrier of 18.91 kcal/mol, and **1,2-F** is lower in free energy by 8.11 kcal/mol in comparison with isolated **D** and 1-hexene. The formation process of **1,2-F** is actually an elementary step of olefin polymerization, which generally features olefin coordination and a four-center insertion transition state. Like the agostic interaction existing in the insertion transition state of olefin polymerization, the coordination of the N atom to the metal plays an important role in stabilizing the structure of **1,2-TS2**. In **1,2-F**, the coordination of the N atom to Sc remained. It is obvious that the 2,1-insertion pathway (blue line in Figure 3) is kinetically and energetically unfavorable in comparison with the 1,2-insertion process because of the higher energy barrier (24.01 kcal/mol) for the former and the lower stability of the resulting

dx.doi.org/10.1021/om300147y | Organometallics 2012, 31, 3930−3937

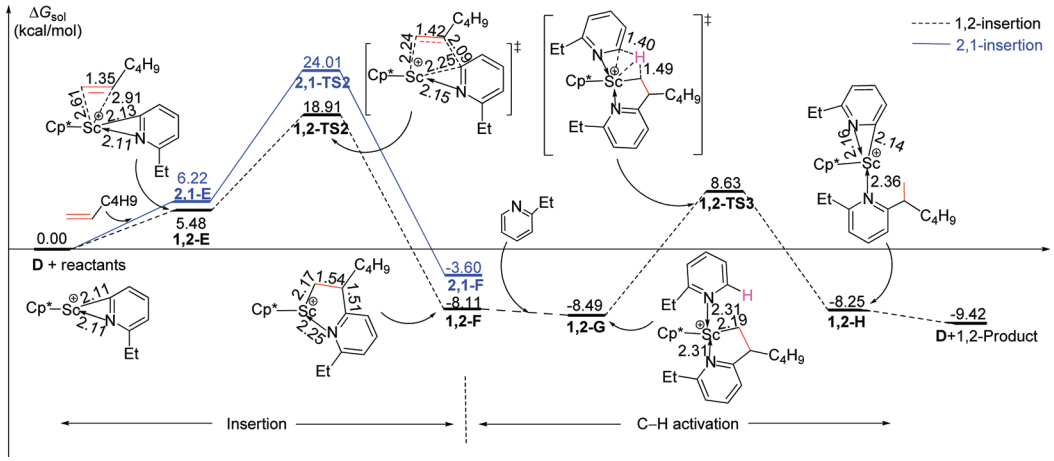

Figure 3. Calculated energy profile (free energy in toluene solution) for insertion and C−H activation processes. The energies are relative to the energy sum of **D**, 1-hexene, and 2-ethylpyridine. The energies of the stationary points involved in the insertion step include the energy of 2-ethylpyridine.

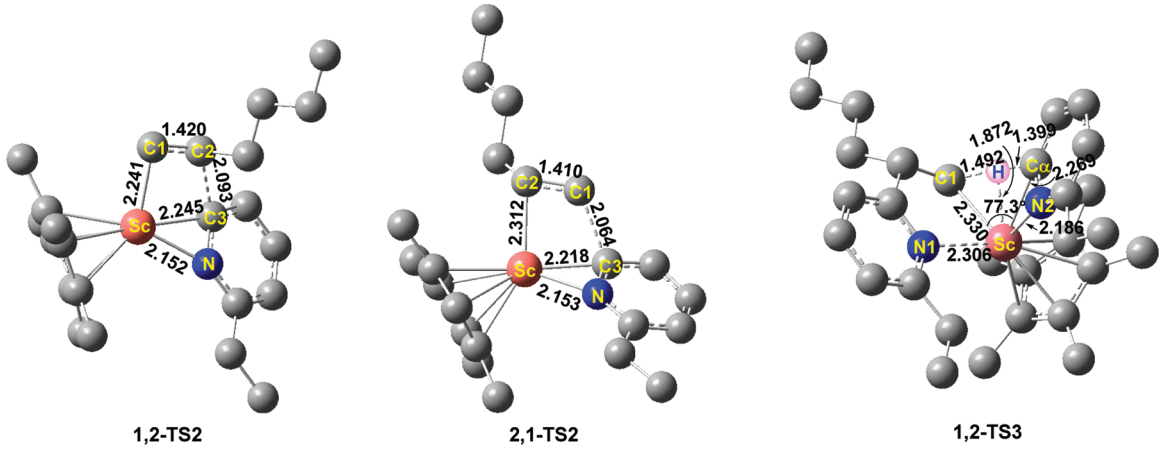

Figure 4. Optimized structures (distances in Å and angles in deg) of **1,2-TS2**, **2,1-TS2**, and **1,2-TS3**. The hydrogens, except for the transferring H, are omitted for clarity.

product **2,1-F**. This result is consistent with experimental observations (Markovnikov C−H addition).[13] In view of the significant priority of the 1,2-insertion process, only **1,2-F** was considered for the calculation of subsequent C−H activation. While the incoming 2-ethylpyridine accesses **1,2-F**, hydrogen transfer from the incoming 2-ethylpyridine to the preinserted pyridine moiety occurs through **1,2-TS3**, which leads to **1,2-H** with a moiety of the newly formed product. The catalytic species **D** can be regenerated via release of the product from **1,2-H**, and the cycle is complete. Like **TS1** shown in Figures 1 and 2, the C−H activation transition state **1,2-TS3** has also a four-center structure involving a transferring H (see the structure of **1,2-TS3** in Figure 4), suggesting a one-step σ-BM process.

In comparison with the zirconium system reported previously,[17] H_2 as a cocatalyst is absent in the current system. The energy profiles for C−H activation and the results of energy decomposition of transition states (see Figure 3S and Table 1S in the Supporting Information) suggest that the metallocene zirconium complex containing two Cp ligands has a more significant steric effect than does the half-metallocene scandium complex. Such a steric effect is crucial in that the zirconium system needs H_2 as a cocatalyst to achieve the catalytic cycle.

1,2-TS3 has a free energy barrier of 17.12 kcal/mol. Such a barrier is slightly lower than that for **1,2-TS2** (18.91 kcal/mol). From the point of view of the whole reaction, the generation of catalytically active species **D** has a slightly higher energy barrier for **TS1** (20.93 kcal/mol, Figure 1) than for either **1,2-TS3** or **1,2-TS2**. Such states, including the intermediate **1,2-F**, could significantly affect the efficiency of the catalytic cycle.[26]

Regioselectivity for the Olefin Insertion. Experimentally, the branched isomer product (Markovnikov C−H addition, 1,2-addition) was obtained exclusively.[13] To access the origin of regioselectivity, the geometrical characters of **1,2-TS2** and **2,1-TS2** are compared. As shown in Figure 4, the Sc−C1 bond length in **1,2-TS2** (2.241 Å) is shorter than the corresponding Sc−C2 bond length in **2,1-TS2** (2.312 Å), whereas C2−C3 in **1,2-TS2** (2.093 Å) is longer than the corresponding C1−C3 bond length in **2,1-TS2** (2.064 Å). It is obvious that these discrepancies are due to the repulsion between the Cp* ligand and $(CH_2)_3CH_3$ group of 1-hexene and that between the pyridine ring and the $(CH_2)_3CH_3$ group, respectively. Such repulsions destabilize **2,1-TS2** and therefore play an important role in regioselectivity. To get deeper insights into the stabilities of the two transition states, energy decomposition analyses (containing BSSE correction) were carried out. It was found that the total deformation energies of

dx.doi.org/10.1021/om300147y | *Organometallics* 2012, 31, 3930−3937

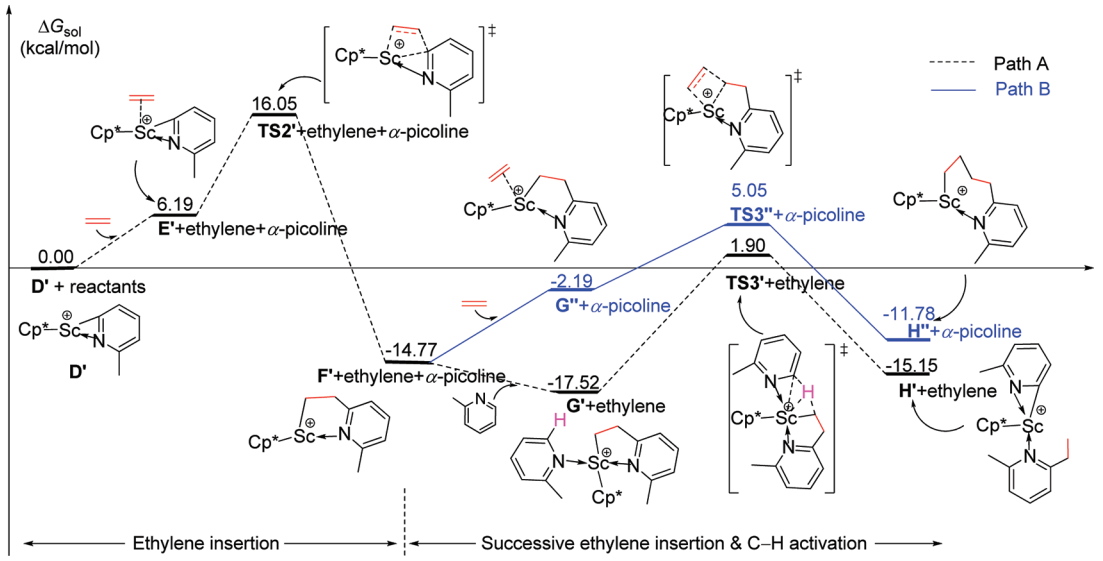

Figure 5. Energy profile (free energy in toluene solution) for ethylene insertion into complex **D′** and subsequent ethylene insertion into complex **F′** as well as α-picoline C−H activation by **F′**. The energies are relative to the energy sum of **D′**, α-picoline, and two molecules of ethylene.

the 1-hexene moiety and active species were 24.35 kcal/mol for **1,2-TS2** and 22.08 kcal/mol for **2,1-TS2**, whereas the interaction energies between the deformed 1-hexene and active species were computed to be −28.73 and −21.76 kcal/mol for **1,2-TS2** and **2,1-TS2**, respectively. This suggests that the interaction between deformed 1-hexene and active species rather than their geometrical deformations plays an important role in the stabilization of the two transition states. Further analyses of charge population indicate that the natural charges on the bonding pair atoms Sc and C1 in **1,2-TS2** are 1.60 and −0.84, respectively. The corresponding charges of 1.62 (Sc) and −0.57 (C2) were found in **2,1-TS2**. These results suggest a stronger electrostatic interaction and hence tighter bonding between Sc and C1 in **1,2-TS2** than that between Sc and C2 in **2,1-TS2**. This is also in line with the shorter Sc−C1 bond length (2.241 Å) in **1,2-TS2** compared with the Sc−C2 bond length of 2.312 Å in **2,1-TS2** (Figure 4). The results shown above suggest that the regioselectivity is governed by both steric and electronic factors.

As shown in Figure 3, the dissociation of the resulting product (2-ethyl-6-isohexylpyridine) from **1,2-H** releases a free energy of 1.17 kcal/mol. Such a situation is a result of a significant entropy contribution, because the electronic energy (containing zero-point correction) required for this dissociation was computed to be 15.43 kcal/mol. On the other hand, the 1,2-coordination of 1-hexene to **D** requires a free energy of 5.48 kcal/mol (Figure 3). Therefore, the replacement of the 2-ethyl-6-isohexylpyridine moiety with 1-hexene in **1,2-H** is endergonic by 5.48 − 1.17 = 4.31 kcal/mol.

Comparison of C−H Activation and Olefin Polymerization. The energy profile for the C−H addition of α-picoline to ethylene has been also computed, and the result is shown in Figure 5. As shown in this figure, such a reaction also occurs via two main steps: an insertion step leading to intermediate **F′** and a C−H activation step leading to **H′**. **H′** could release the resulting product to regenerate the active species **D′** (the energy profile for the formation of **D′** is shown in Figure 1S in the Supporting Information). Previous experimental results showed that cationic half-sandwich rare-earth alkyl complexes can serve as excellent catalysts for the polymerization and copolymerization of a variety of olefins.[11,12] However, the cationic scandium catalyst $(\eta^5\text{-}C_5Me_5)Sc(CH_2C_6H_4NMe_2\text{-}o)^+$ cannot polymerize ethylene in the presence of pyridines, and ethylene polymerization could only take place after the pyridines were completely consumed.[13] To add a better molecular-level understanding to this observation, the energy profiles for the successive insertion of ethylene into **F′** have also been computed here and the result is also included in Figure 5 (path B in blue) for comparison. As shown in Figure 5, the coordination of an ethylene to **F′** is endergonic by 12.58 kcal/mol, while the coordination of an α-picoline to the same intermediate is exergonic by 2.75 kcal/mol. The ethylene insertion product **H″** (path B) is higher in free energy by 3.37 kcal/mol in comparison with **H′** derived from pyridine C−H activation (path A). These results suggest that not only the favorable coordination of pyridine to the metal center but also the energetic preference for the formation of a C−H activation product made path A more favorable than path B (Figure 5). The transition states **TS3″** and **TS3′** have similar free energy barriers, viz. 19.82 and 19.42 kcal/mol, respectively. However, **TS3′** has a lower relative energy (1.90 kcal/mol) than **TS3″** (5.05 kcal/mol), suggesting a slightly kinetic preference for pyridyl C−H activation in path A. It is the significant thermodynamic advantage of the complex **G′** in comparison with **G″** that could suppress the successive ethylene insertion/polymerization in the presence of pyridine. As the free energy barrier for **TS3″** (19.82 kcal/mol) is accessible, the ethylene polymerization could occur in the absence of α-picoline in this reaction system.

Comparison of the Induction Periods for Ethylene Polymerization by $(\eta^5\text{-}C_5Me_5)Sc(CH_2C_6H_4NMe_2\text{-}o)^+$ (A) and $(\eta^5\text{-}C_5Me_5)Sc(MeC_5H_3N)^+$ (D). It was reported that the cationic species $(\eta^5\text{-}C_5Me_5)Sc(CH_2C_6H_4NMe_2\text{-}o)^+$ (**A**)[12d] and $(\eta^5\text{-}C_5Me_5)Sc(MeC_5H_3N)^+$ (**D′**)[13] (in the absence of pyridine) could both catalyze the polymerization of ethylene. In view of the structural similarity of **D′** and **A**, the effects of alkyl groups in the two cationic species on the chain initiation of ethylene polymerization have been computationally investigated. The results are shown in Figure 6, where routes 1 and 2 are for **D′** and **A**, respectively. As shown in this figure, the coordination

dx.doi.org/10.1021/om300147y | Organometallics 2012, 31, 3930−3937

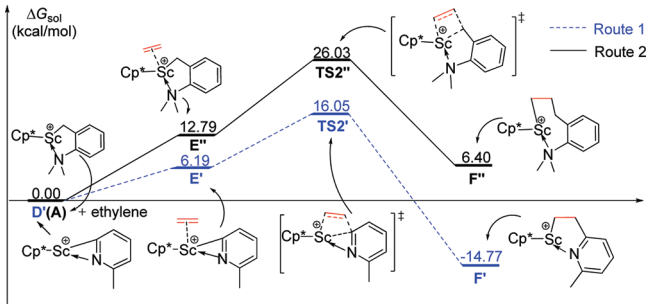

Figure 6. Energy profile (free energy in toluene solution) for the chain initiation of ethylene polymerization catalyzed by $(\eta^5\text{-}C_5Me_5)Sc(CH_2C_6H_4NMe_2\text{-}o)^+$ (**A**) and $(\eta^5\text{-}C_5Me_5)Sc(MeC_5H_3N)^+$ (**D′**).

complexes **E′** (route 1) is lower in energy than **E″** (route 2) by 6.6 kcal/mol. Such coordination complexes (**E′** and **E″**) are higher in free energy in comparison with the isolated species (cation + ethylene) because of entropy contributions. The ethylene insertion process along with routes 1 and 2 proceed by four-center transition states, **TS2′** and **TS2″**, which overcome free energy barriers of 16.05 and 26.03 kcal/mol, respectively. The corresponding product **F′** is significantly more stable (−14.77 kcal/mol) than **F″** (6.40 kcal/mol). These results indicate that route 1 is more favorable than route 2 both kinetically and energetically. In this sense, we predict that the induction period for the **D′**-catalyzed ethylene polymerization is shorter than that for the **A**-catalyzed process.

Comparison of the sp³ and sp² C−H Activation and Subsequent Olefin Insertion. In a previous communication,[13] an experimental observation was noted. That is, deuterium labeling experiments showed that alkylation of 2-methyl-6-deuteriopyridine with ethylene or styrene in the presence of $(C_5Me_5)Ln(CH_2C_6H_4NMe_2\text{-}o)_2$ (Ln = Sc, Y)/$B(C_6F_5)_3$ in toluene at 70 °C gave the corresponding ortho-alkylation products with partial deuteration at both the *o*-methyl group and the *β*-carbon atom. In the absence of an olefin, H/D exchange between the methyl C−H and the pyridyl C−D units was observed. In order to get a better understanding of this experimental observation, the energy profile for the reaction of *α*-picoline with cationic complex **A**, leading to species **D′** (resulting from the activation of the aromatic ring sp² C−H bond) and **Da** (resulting from the activation of the methyl sp³ C−H bond), has been computed (Figure 7). The formation of **D′** is also shown in Figure 1S in the Supporting Information. As shown in Figure 7, both processes occurred via four-center transition states. In comparison with the aforementioned structure **TS1**, **TS1′** and **TS1a** have similar geometrical characters (see Figure 2S in the Supporting Information), suggesting a *σ*-BM mechanism. It is obvious that the free energy barrier of **TS1′** (20.83 kcal/mol) is lower than that of **TS1a** (24.73 kcal/mol) and the free energy of **C′** (2.90 kcal/mol) is lower than that of **Ca** (4.47 kcal/mol), which means that the activation of the sp² C−H bond is more favorable in comparison to the activation of the methyl sp³ C−H bond in this step. This result is in line with previous theoretical studies on the reaction of the C−H activation of *α*-picoline by $(C_5Me_5)_2U(CH_3)_2$.[27,28] The species **D′** could be transformed into **Da** by its reaction with another molecule of *α*-picoline. The computed energy profile for this transformation (from **D′** to **Da**) is shown in Figure 8.

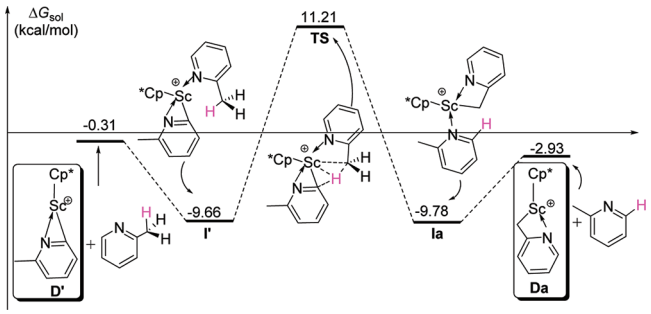

Figure 8. Energy profile (free energy in toluene solution) for the conversion of **D′** and **Da**. The energies are relative to the energy sum of **A** and two molecules of *α*-picoline, and the energy of each stationary point includes the energy of *o*-$Me_2NC_6H_4Me$.

As shown in Figure 8, the reaction of **D′** with *α*-picoline yields complex **I′** and then goes through a four-center HT transition state (*σ*-BM), **TS**, leading to the formation of complex **Ia**. The **Ia** could release *α*-picoline to give the species **Da**. The **TS** has a free energy barrier of 20.87 kcal/mol, which is lower than that of **TS1a** (24.73 kcal/mol shown in Figure 7). Therefore, we infer that **Da** mainly results from the conversion of **D′** in the presence of *α*-picoline rather than from the direct reaction of **A** with *α*-picoline in this reaction. **I′** and **Ia** (in Figure 8), which connect **TS**, have almost the same thermal

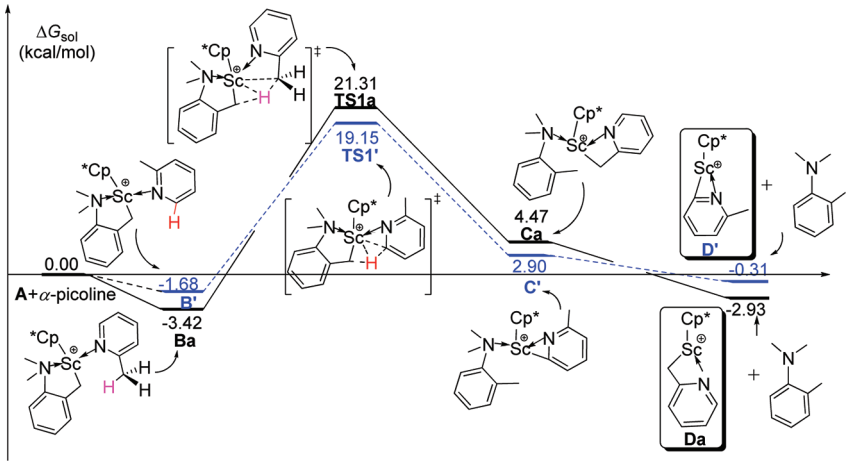

Figure 7. Energy profile (free energy in toluene solution) for the formation of species **D′** and **Da** via the reaction of **A** with *α*-picoline.

dx.doi.org/10.1021/om300147y | *Organometallics* 2012, 31, 3930−3937

stability. This suggests that the conversion of **I′** and **Ia** is reversible and **D′** and **Da** coexist in the reaction system. In other words, in the absence of an olefin, **D′** and **Da** are in dynamic equilibrium (eq 1). It is because of the reversibility of

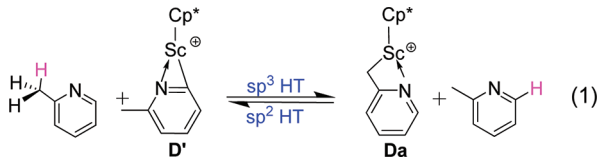

(1)

this reaction that the H/D exchange between the methyl C−H and the pyridyl C−D units as well as ortho-alkylation products with partial deuteration were observed experimentally.

It should be noted that the release of α-picoline from **I′** requires a free energy of 9.35 kcal/mol (Figure 8), and the coordination of ethylene to **D′** is endergonic by 6.19 kcal/mol (Figures 5 and 6). Therefore, the replacement of α-picoline with ethylene in **I′** is endergonic by 15.54 kcal/mol. The whole process, however, is exergonic by 15.15 kcal/mol (Figure 5). Considering this and the insertion energy barrier of 16.06 kcal/mol (Figure 5), the replacement of α-picoline with ethylene and subsequent olefin insertion are slow, but they are accessible with respect to the moderate energy barrier and experimental conditions (70 °C, 3 atm of ethylene).[13] Such an endergonic character of the replacement of α-picoline with olefin at the metal center was also found in the analogous Zr system.[17]

Considering that **Da** might also be involved in the catalytic cycle, the catalytic pathway for the reaction of **Da** with ethylene has been computed (black line in Figure 9). For comparison, the energy profile for the reaction of ethylene with **D′** (shown in Figure 5) is also included in Figure 9 (blue line). As shown in this figure, **TS2′** and **TS2a** have energy barriers of 16.05 and 18.91 kcal/mol, respectively, and **F′** is significantly lower in free energy by 9.40 kcal/mol in comparison with **Fa**. This suggests that the insertion of olefin into **Da** is energetically unfavorable in comparison with that into **D′**. To corroborate this result, calculations at the level of B3LYP, BP86, and MPW1K theories have been also performed, and consistent results were obtained (see Figures 4S−6S in the Supporting Information). Therefore, the olefins mainly react with **D′** rather than **Da** in the catalytic cycle. This result is consistent with the experimental observation that the alkylation product is 2-methyl-6-ethylpyridine instead of 2-propylpyridine.

As shown in Figure 9, the reaction of incoming α-picoline with the resulting **F′** has also two paths for C−H activation: the activation of the aromatic ring sp^2 C−H bond (sp^2 path) and the activation of the methyl sp^3 C−H bond (sp^3 path). The sp^2 and sp^3 paths have energy barriers of 19.42 and 20.39 kcal/mol, respectively, and complex **H′** resulting from the sp^2 path is lower in free energy by 1.49 kcal/mol in comparison with **Ha**. This suggests that the sp^2 path is favorable over the sp^3 path.

On the basis of computations, the mechanism for the Sc-catalyzed C−H addition of pyridines to olefins is illustrated in Scheme 2. The C−H bond activation of pyridine in both process a and process b occurred via the activation of the aromatic ring sp^2 C−H bond instead of the activation of the alkyl sp^3 C−H bond. **Da** (sp^3 intermediate) is mainly formed by the conversion of **D′** (sp^2 intermediate) rather than the direct reaction of **A** with pyridine, and the reaction from **D′** to **Da** is reversible. Due to this reversibility, H/D exchange between the methyl C−H and the pyridyl C−D units was observed in deuterium labeling experiments. In the catalytic

Scheme 2. Complete Reaction Process of Sc-Catalyzed C−H Addition of Pyridines to Olefins

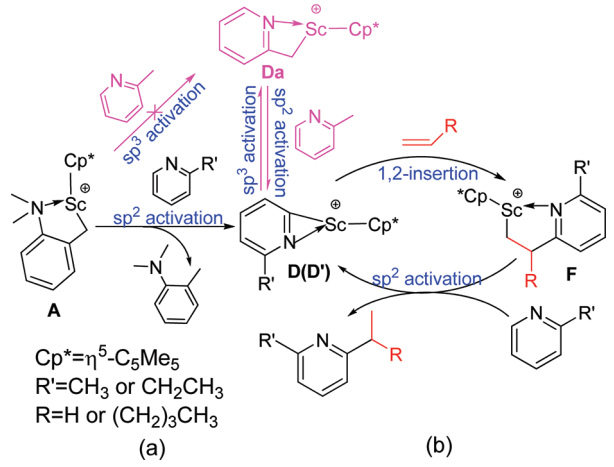

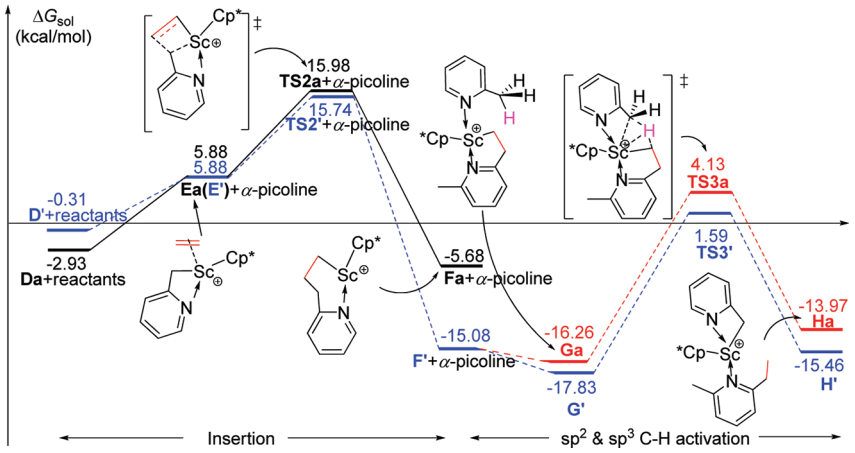

Figure 9. Energy profile (free energy in toluene solution) for ethylene insertion into complexes **D′** and **Da** and α-picoline C−H activation by **F′**. The structures **E′**−**H′** refer to Figure 5. The energies are relative to the energy sum of **A**, ethylene, and two molecules of α-picoline, and the energy of each stationary point includes the energy of *o*-$Me_2NC_6H_4Me$.

dx.doi.org/10.1021/om300147y | *Organometallics* 2012, 31, 3930−3937

cycle, olefin reaction with **D′** is more favorable in comparison with **Da**.

CONCLUSIONS

The Sc-catalyzed addition of the *o*-C−H bond of pyridine derivatives to olefins has been investigated by DFT calculations. The computational results support the proposed mechanism, which mainly involves two processes: (a) the formation of active intermediates and (b) the process of catalyzing C−H addition of pyridines to olefins. The latter includes two steps: coordination and insertion of olefin and the metal-mediated C−H activation of pyridines. In addition, it has been also computationally found that the methyl sp^3 C−H activation product of α-picoline mainly results from the conversion of the sp^2 C−H activation product of α-picoline rather than from the direct reaction of the cationic species $(\eta^5\text{-}C_5Me_5)Sc(CH_2C_6H_4NMe_2\text{-}o)^+$ with α-picoline, and such a conversion is reversible. The scandium-catalyzed C−H bond addition of 2-ethylpyridine to 1-hexene preferably yields the 1,2-insertion product. Both steric and electronic factors control the regioselectivity in the current system. Interestingly, the energy analyses of the 1,2- and 2,1-insertion transition states of 1-hexene indicate that the interaction energy between the 1-hexene moiety and active species rather than their deformations plays an important role in the stabilization of such transition states. The competition between olefin polymerization and pyridine C−H activation were also investigated in this study. It has been found that the coordination of α-picoline to the metal center is significantly favorable in comparison with that of ethylene, which could suppress ethylene polymerization in the presence of α-picoline. In addition, it is predicted that the cationic species $(\eta^5\text{-}C_5Me_5)Sc(MeC_5H_3N)^+$ has a shorter induction period than $(\eta^5\text{-}C_5Me_5)Sc(CH_2C_6H_4NMe_2\text{-}o)^+$ for the chain-initiation stage of ethylene polymerization.

ASSOCIATED CONTENT

Supporting Information

Figures and tables giving energy profiles for the formation of **D′**, insertion of ethylene into complex **D′** (**Da**) computed at the B3LYP, BP86 and MPW1K levels, energy decomposition analyses, optimized structures of transition states **TS1′** and **TS1a**, and Cartesian coordinates of optimized stationary points. This material is available free of charge via the Internet at http://pubs.acs.org.

AUTHOR INFORMATION

Corresponding Author

*E-mail: luoyi@dlut.edu.cn (Y.L.); houz@riken.jp (Z.H.).

Notes

The authors declare no competing financial interest.

ACKNOWLEDGMENTS

This work was supported by the National Natural Science Foundation of China (Nos. 21028001, 21174023, 21137001). Y.L. thanks the SEM Scientific Research Funding for ROCS. Z.H. acknowledges financial support from China's Thousand Talents Program.We also thank the RICC (RIKEN Integrated Cluster of Clusters) and the Network and Information Center of the Dalian University of Technology for some computational resources.

REFERENCES

(1) (a) Michael, J. P. *Nat. Prod. Rep.* **2005**, *22*, 627−646. (b) Henry, G. D. *Tetrahedron* **2004**, *60*, 6043−6061. (c) Bagley, M. C.; Glover, C.; Merritt, E. A. *Synlett* **2007**, 2459−2482. (d) Arena, C. G.; Arico, G. *Curr. Org. Chem.* **2010**, *14*, 546−580. (e) Bianchini, C.; Giambastiani, G.; Luconi, L.; Meli. *A. Coord. Chem. Rev.* **2010**, *254*, 431−455. (f) Holliday, B. J.; Mirkin, C. A. *Angew. Chem., Int. Ed.* **2001**, *40*, 2022−2043. (g) Kurth, D. G.; Higuchi, M. *Soft Matter* **2006**, *2*, 915−927.

(2) A recent review: Nakao, Y. *Synthesis* **2011**, *20*, 3209−3219.

(3) For examples of borylation, see: (a) Cho, J.; Iverson, C. N.; Smith, M. R. *J. Am. Chem. Soc.* **2000**, *122*, 12868−12869. (b) Takagi, J.; Sato, K.; Hartwig, J. F.; Ishiyama, T.; Miyaura, N. *Tetrahedron Lett.* **2002**, *43*, 5649−5651. (c) Mkhalid, I. A. I.; Coventry, D. N.; Albesa-Jove, D.; Batsanov, A. S.; Howard, J. A. K.; Perutz, R. N.; Marder, T. B. *Angew. Chem., Int. Ed.* **2006**, *45*, 489−491. (d) Murphy, J. M.; Liao, X.; Hartwig, J. F. *J. Am. Chem. Soc.* **2007**, *129*, 15434−15435. (e) Fischer, D. F.; Sarpong, R. *J. Am. Chem. Soc.* **2010**, *132*, 5926−5927. (f) Hurst, T. E.; Macklin, T. K.; Becker, M.; Hartmann, E.; Gel, W. K.; Salle, J. P.; Batsanov, A. S.; Marder, T. B.; Snieckus, V. *Chem. Eur. J.* **2010**, *16*, 8155−8161.

(4) For examples of arylation, see: (a) Godula, K.; Sezen, B.; Sames, D. *J. Am. Chem. Soc.* **2005**, *127*, 3648−3649. (b) Berman, A. M.; Lewis, J. C.; Bergman, R. G.; Ellman, J. A. *J. Am. Chem. Soc.* **2008**, *130*, 14926−14927. (c) Tobisu, M.; Hyodo, I.; Chatani, N. *J. Am. Chem. Soc.* **2009**, *131*, 12070−12071. (d) Yanagisawa, S.; Ueda, K.; Taniguchi, T.; Itami, K. *Org. Lett.* **2008**, *10*, 4673−4676. (e) Kobayashi, O.; Uraguchi, D.; Yamakawa, T. *Org. Lett.* **2009**, *11*, 2679−2682. (f) Li, M.; Hua, R. *Tetrahedron Lett.* **2009**, *50*, 1478−1481. (g) Seiple, I. B.; Su, S.; Rodriguez, R. A.; Gianatassio, R.; Fujiwara, Y.; Sobel, A. L.; Baran, P. S. *J. Am. Chem. Soc.* **2010**, *132*, 13194−13196.

(5) For examples of olefination, see: (a) Murakami, M.; Hori, S. *J. Am. Chem. Soc.* **2003**, *125*, 4720−4721. (b) Nakao, Y.; Kanyiva, K. S.; Hiyama, T. *J. Am. Chem. Soc.* **2008**, *130*, 2448−2449. (c) Tsai, C.; Shih, W.; Fang, C.; Li, C.; Ong, T.; Yap, G. P. A. *J. Am. Chem. Soc.* **2010**, *132*, 11887−11889. (d) Ye, M.; Gao, G.; Yu, J. *J. Am. Chem. Soc.* **2011**, *133*, 6964−6967.

(6) For some other examples, see: (a) Moore, E. J.; Pretzer, W. R.; O'Connell, T. J.; Harris, J.; LaBounty, L.; Chou, L.; Grimmer, S. S. *J. Am. Chem. Soc.* **1992**, *114*, 5888−5890. (b) Kawashima, T.; Takao, T.; Suzuki, H. *J. Am. Chem. Soc.* **2007**, *129*, 11006−11007. (c) Beveridge, R. E.; Arndtsen, B. A. *Synthesis* **2010**, 1000−1008. (d) Tran, L. D.; Daugulis, O. *Org. Lett.* **2010**, *12*, 4277−4279. (e) Li, B.; Shi, Z. *Chem. Sci.* **2011**, *2*, 488−493. (f) Correia, C. A.; Yang, L.; Li, C. *Org. Lett.* **2011**, *13*, 4581−4583.

(7) (a) Jordan, R. F.; Taylor, D. F. *J. Am. Chem. Soc.* **1989**, *111*, 778−779. (b) Jordan, R. F.; Taylor, D. F.; Baenziger, N. C. *Organometallics* **1990**, *9*, 1546−1557. (c) Rodewald, S.; Jordan, R. F. *J. Am. Chem. Soc.* **1994**, *116*, 4491−4492. (d) Guram, A. S.; Jordan, R. F. *Organometallics* **1991**, *10*, 3470−3479. (e) Dagorne, S.; Rodewald, S.; Jordan, R. F. *Organometallics* **1997**, *16*, 5541−5555.

(8) (a) Lewis, J. C.; Bergman, R. G.; Ellman, J. A. *J. Am. Chem. Soc.* **2007**, *129*, 5332−5333. (b) Yotphan, S.; Bergman, R. G.; Ellman, J. A. *Org. Lett.* **2010**, *12*, 2978−2981.

(9) Nakao, Y.; Yamada, Y.; Kashihara, N.; Hiyama, T. *J. Am. Chem. Soc.* **2010**, *132*, 13666−13668.

(10) (a) Deelman, B.; Stevels, W. M.; Teuben, J. H.; Lakin, M. T.; Spek, A. L. *Organometallics* **1994**, *13*, 3881−3891. (b) Duchateau, R.; Brussee, E. A. C.; Meetsma, A.; Teuben, J. H. *Organometallics* **1997**, *16*, 5506−5516. (c) Carver, C. T.; Diaconescu, P. L. *J. Alloys Compd.* **2009**, *488*, 518−523.

(11) Selected reviews: (a) Nishiura, M.; Hou, Z. *Nature Chem.* **2010**, *2*, 257−268. (b) Rodrigues, A. S.; Carpentier, J. F. *Coord. Chem. Rev.* **2008**, *252*, 2137−2154. (c) Li, X.; Hou, Z. *Coord. Chem. Rev.* **2008**, *252*, 1842−1869. (d) Zeimentz, P. M.; Arndt, S.; Elvidge, B. R.; Okuda, J. *Chem. Rev.* **2006**, *106*, 2404−2433. (e) Kretschmer, W. P.; Meetsma, A.; Hessen, B.; Schmalz, T.; Sadaf, Q.; Kempe, R. *Chem. Eur. J.* **2006**, *12*, 8969−8978. (f) Hou., Z.; Wakatsuki, Y. *Coord. Chem. Rev.* **2002**, *231*, 1−22. (g) Evans, W. J.; Davis, B. L. *Chem. Rev.* **2002**, *102*,

2119−2136. (h) Marques, M.; Sella, A.; Takats, J. *Chem. Rev.* **2002**, *102*, 2137−2160. (i) Chen, E. Y. X.; Marks, T. J. *Chem. Rev.* **2000**, *100*, 1391−1434.
(12) (a) Luo, Y.; Baldamus, J.; Hou, Z. *J. Am. Chem. Soc.* **2004**, *126*, 13910−13911. (b) Li, X.; Hou, Z. *Macromolecules* **2005**, *38*, 6767−6769. (c) Li, X. F.; Baldamus, J.; Nishiura, M.; Tardif, O.; Hou, Z. M. *Angew. Chem., Int. Ed.* **2006**, *45*, 8184−8188. (d) Li, X. F.; Nishiura, M.; Mori, K.; Mashiko, T.; Hou, Z. M. *Chem. Commun.* **2007**, 4137−4139. (e) Yu, N.; Nishiura, M.; Li, X. F.; Xi, Z. F.; Hou, Z. M. *Chem. Asian J.* **2008**, *3*, 1406−1414. (f) Zhang, H.; Luo, Y.; Hou, Z. *Macromolecules* **2008**, *41*, 1064−1066. (g) Li, X.; Nishiura, M.; Hu, L.; Mori, K.; Hou, Z. *J. Am. Chem. Soc.* **2009**, *131*, 13870−13882. (h) Li, X.; Hou, Z. *Macromolecules* **2010**, *43*, 8904−8909. (i) Pan, L.; Zhang, K.; Nishiura, M.; Hou, Z. *Macromolecules* **2010**, *43*, 9591−9593. (j) Guo, F.; Nishiura, M.; Koshino, H.; Hou, Z. *Macromolecules* **2011**, *44*, 6335−6344. (k) Guo, F.; Nishiura, M.; Koshino, H.; Hou, Z. *Macromolecules* **2011**, *44*, 2400−2403. (l) Pan, L.; Zhang, K.; Nishiura, M.; Hou, Z. *Angew. Chem., Int. Ed.* **2011**, *50*, 12012−12015.
(13) Guan, B.; Hou, Z. *J. Am. Chem. Soc.* **2011**, *133*, 18086−18089.
(14) (a) Foley, N. A.; Lee, J. P.; Ke, Z.; Gunnoe, T. B.; Cundari, T. R. *Acc. Chem. Res.* **2009**, *42*, 585−597. (b) McKeown, B. A.; Gonzalez, H. E.; Friedfeld, M. R.; Gunnoe, T. B.; Cundari, T. R.; Sabat, M. *J. Am. Chem. Soc.* **2011**, *133*, 19131−19152. (c) Lail, M.; Bell, C. M.; Conner, D.; Cundari, T. R.; Gunnoe, T. B.; Petersen, J. L. *Organometallics* **2004**, *23*, 5007−5020.
(15) Andreatta, J. R.; McKeown, B. A.; Gunnoe, T. B. *J. Organomet. Chem.* **2011**, *696*, 305−315.
(16) (a) Oxgaard, J.; Muller, R. P.; Goddard, W. A.; Periana, R. A. *J. Am. Chem. Soc.* **2004**, *126*, 352−363. (b) Oxgaard, J.; Goddard, W. A. *J. Am. Chem. Soc.* **2004**, *126*, 442−443. (c) Oxgaard, J.; Periana, R. A.; Goddard, W. A. *J. Am. Chem. Soc.* **2004**, *126*, 11658−11665. (d) Bhalla, G.; Oxgaard, J.; Goddard, W. A.; Periana, R. A. *Organometallics* **2005**, *24*, 3229−3232.
(17) Bi, S.; Lin, Z.; Jordan, R. F. *Organometallics* **2004**, *23*, 4882−4890.
(18) Selected examples: (a) Luo, Y.; Selvam, P.; Endou, A.; Kubo, M.; Miyamoto, A. *J. Am. Chem. Soc.* **2003**, *125*, 16210−16212. (b) Luo, Y.; Selvam, P.; Ito, Y.; Takami, S.; Kubo, M.; Imamura, A.; Miyamoto, A. *Organometallics* **2003**, *22*, 2181−2183. (c) Luo, Y.; Baldamus, J.; Tardif, O.; Hou, Z. *Organometallics* **2005**, *24*, 4362−4366. (d) Luo, Y.; Hou, Z. *Organometallics* **2007**, *26*, 2941−2944. (e) Luo, Y.; Hou, Z. *Int. J. Quantum Chem.* **2007**, *107*, 374−381. (f) Luo, Y.; Hou, Z. *J. Phys. Chem. C* **2008**, *112*, 635−638. (g) Shima, T.; Luo, Y.; Stewart, T.; Bau, R.; McIntyre, G. J.; Mason, S. A.; Hou, Z. *Nature Chem.* **2011**, *3*, 814−820. (h) Luo, Y.; Li, Y.; Yu, H.; Zhao, J.; Chen, Y.; Hou, Z.; Qu, J. *Organometallics* **2012**, *31*, 335−344.
(19) (a) Zhang, L.; Suzuki, T.; Luo, Y.; Nishiura, M.; Hou, Z. *Angew. Chem., Int. Ed.* **2007**, *46*, 1909−1913. (b) Zhang, L.; Luo, Y.; Hou, Z. *J. Am. Chem. Soc.* **2005**, *127*, 14562−14563. (c) Luo, Y.; Hou, Z. *Organometallics* **2006**, *25*, 6162−6165. (d) Luo, Y.; Luo, Y.; Qu, J.; Hou, Z. *Organometallics* **2011**, *30*, 2908−2919. (e) Kang, X.; Song, Y.; Luo, Y.; Li, G.; Hou, Z.; Qu, J. *Macromolecules* **2012**, *45*, 640−651.
(20) Frisch, M. J.; Trucks, G. W.; Schlegel, H. B.; Scuseria, G. E.; Robb, M. A.; Cheeseman, J. R.; Scalmani, G.; Barone, V.; Mennucci, B.; Petersson, G. A.; Nakatsuji, H.; Caricato, M.; Li, X.; Hratchian, H. P.; Izmaylov, A. F.; Bloino, J.; Zheng, G.; Sonnenberg, J. L.; Hada, M.; Ehara, M.; Toyota, K.; Fukuda, R.; Hasegawa, J.; Ishida, M.; Nakajima, T.; Honda, Y.; Kitao, O.; Nakai, H.; Vreven, T.; Montgomery, , J. A., Jr.; Peralta, J. E.; Ogliaro, F.; Bearpark, M.; Heyd, J. J.; Brothers, E.; Kudin, K. N.; Staroverov, V. N.; Kobayashi, R.; Normand, J.; Raghavachari, K.; Rendell, A.; Burant, J. C.; Iyengar, S. S.; Tomasi, J.; Cossi, M.; Rega, N.; Millam, N. J.; Klene, M.; Knox, J. E.; Cross, J. B.; Bakken, V.; Adamo, C.; Jaramillo, J.; Gomperts, R.; Stratmann, R. E.; Yazyev, O.; Austin, A. J.; Cammi, R.; Pomelli, C.; Ochterski, J. W.; Martin, R. L.; Morokuma, K.; Zakrzewski, V. G.; Voth, G. A.; Salvador, P.; Dannenberg, J. J.; Dapprich, S.; Daniels, A. D.; Farkas, Ö.; Foresman, J. B.; Ortiz, J. V.; Cioslowski, J.; Fox, D. J. *Gaussian 09, Revision A.02*; Gaussian, Inc., Wallingford, CT, 2009.
(21) (a) Beck, A. D. *J. Chem. Phys.* **1993**, *98*, 5648−5652. (b) Lee, C. T.; Yang, W. T.; Parr, R. G. *Phys. Rev. B* **1988**, *37*, 785−789. (c) Perdew, J. P.; Burke, K.; Wang, Y. *Phys. Rev. B* **1996**, *54*, 16533−16539.
(22) (a) Dolg, M.; Wedig, U.; Stoll, H.; Preuss, H. *J. Chem. Phys.* **1987**, *86*, 866−872. (b) Schwerdtfeger, P.; Dolg, M.; Schwarz, W. H. E.; Bowmaker, G. A.; Boyd, P. D. W. *J. Chem. Phys.* **1989**, *91*, 1762−1774. (c) Dolg, M.; Stoll, H.; Savin, A.; Preuss, H. *Theor. Chim. Acta* **1989**, *75*, 173−194. (d) Andrae, D.; Haeussermann, U.; Dolg, M.; Stoll, H.; Preuss, H. *Theor. Chim. Acta* **1990**, *77*, 123−141. (e) Dolg, M.; Stoll, H.; Preuss, H. *Theor. Chim. Acta* **1993**, *85*, 441−450. (f) Bergner, A.; Dolg, M.; Kuechle, W.; Stoll, H.; Preuss, H. *Mol. Phys.* **1993**, *80*, 1431−1441.
(23) (a) Miertus, S.; Scrocco, E.; Tomasi, J. *Chem. Phys.* **1981**, *55*, 117−129. (b) Cammi, R.; Mennucci, B.; Tomasi, J. *J. Phys. Chem. A* **2000**, *104*, 5631−5637.
(24) (a) Luft, J. A. R.; Meleson, K.; Houk, K. N. *Org. Lett.* **2007**, *9*, 555−558. (b) Dobereiner, G. E.; Nova, A.; Schley, N. D.; Hazari, N.; Miller, S. J.; Eisenstein, O.; Crabtree, R. H. *J. Am. Chem. Soc.* **2011**, *133*, 7547−7562. (c) Nova, A.; Balcells, D.; Schley, N. D.; Dobereiner, G. E.; Crabtree, R. H.; Eisenstein, O. *Organometallics* **2010**, *29*, 6548−6558.
(25) (a) Vastine, B. A.; Hall, M. B. *Coord. Chem. Rev.* **2009**, *253*, 1202−1218. (b) Lin, Z. *Coord. Chem. Rev.* **2007**, *251*, 2280−2291. (c) Lin, Z. *Acc. Chem. Res.* **2010**, *43*, 602−611.
(26) Kozuch, S.; Shaik, S. *Acc. Chem. Res.* **2011**, *44*, 101−110.
(27) Yang, P.; Warnke, I.; Martin, R. L.; Hay, P. J. *Organometallics* **2008**, *27*, 1384−1392.
(28) Castro, L.; Yahia, A.; Maron, L. *Dalton Trans.* **2010**, *39*, 6682−6692.